Theory of quantum-enhanced spectroscopy with general Markovian light sources

Erfan Abbasgholinejad

A thesis
submitted in partial fulfillment of the
requirements for the degree of

Master of Science in Electrical Engineering

University of Washington

2024

Reading Committee:

Rahul Trivedi, Chair

Arka Majumdar

Program Authorized to Offer Degree:

Department of Electrical and Computer Engineering

University of Washington

Abstract

Theory of quantum-enhanced spectroscopy with general Markovian light sources

Erfan Abbasgholinejad

Chair of the Supervisory Committee:
Assistant Professor Rahul Trivedi
Department of Electrical and Computer Engineering

Photonic states, such as NOON states and super-radiant states, are potentially useful for quantum-enhanced spectroscopy. However, generating these specific states, which are known to provide a quantum advantage, can be experimentally challenging. While several light sources, often comprising of multiple quantum emitters interacting with engineered optical modes, can be used to generate non-classical states of light, whether or not these states have quantum metrological potential remains less well understood. In this work, we develop a general framework to analyze quantum enhanced spectroscopy with generalized Markovian light sources. *First*, by exploiting a matrix-product state representation of the emitted photon state, we relate its quantum Fisher Information (QFI) in a spectroscopy setup to the Lindbladian governing the internal dynamics of the light source. We also use this relationship to elucidate the connection between the Lindbladian spectrum and the possibility of a quantum metrological advantage. *Finally*, we construct the optimal measurement (i.e. measurement saturating the quantum Cramer Rao bound) that requires reabsorption of photons into a controllable auxiliary system and time-local photodetection.

TABLE OF CONTENTS

LIST OF FIGURES

ACKNOWLEDGMENTS

First, I want to extend my deepest gratitude to my advisor, Rahul Trivedi, for his invaluable supervision and guidance. His brilliance, constant availability and unwavering support have been crucial in shaping me as a researcher. I would also like to thank Arka Majumdar for graciously agreeing to be on my committee. Finally, I am deeply thankful to all my friends, and especially my family, for their support throughout this journey.

Chapter 1

INTRODUCTION

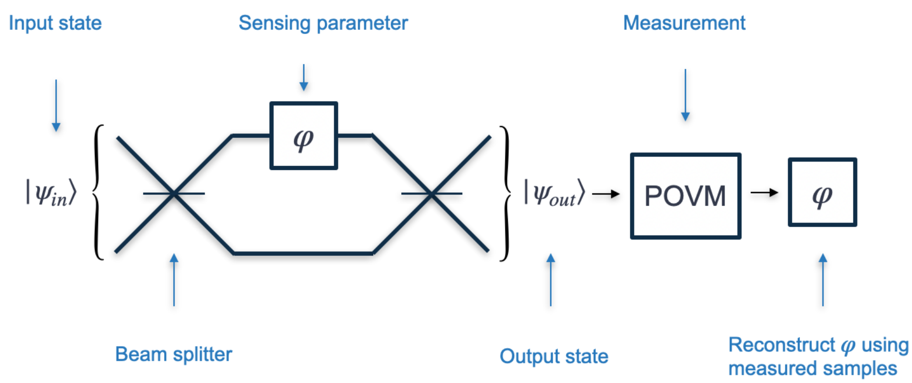

Figure 1.1: Schematic depiction of an inteferometry set up. The input photonic state passes though a MZI that includes an unknown sensing parameter, φ. The objective is to apply a Positive Operator-Valued Measure (POVM) on the output state and reconstruct φ based on the measurement outcomes.

The foundation of utilizing light in metrology lies in interference. In a Mach-Zender Interferometer (MZI) setup (Fig. 1.1), comprising two light paths, one can measure the phase difference of the two arms φ by causing interference between the light traversing both paths. In a semi-classical depiction, the measurement error in φ is influenced by the Poisson distribution of photon counts at the output. This error, known as the Shot-Noise-Limit (SNL), is proportionate to $\delta\varphi \geq 1/\sqrt{N}$, with N representing the average number of photons utilized for the phase measurement. In a quantum framework, exploiting entanglement and correlations between the two light paths becomes possible. Instead of employing coherent states in both paths, initiating with a quantum state of photons, such as twin Fock states, allows for an enhanced measurement of the relative phase difference of the MZI arms. Studies have demonstrated that the error in this scenario is constrained by $\delta\varphi \geq 1/N$, recognized as the Heisenberg-Limit (HL) [1].

In general, generating quantum states of light that are known to exhibit quantum advantage, such as twin Fock states and NOON states with deterministic photon numbers, poses a considerable challenge. Consequently, researchers have explored more experimentally relevant quantum states for metrology by investigating states created through the emission of multiple emitters into optical modes. Notably, studies have revealed that quantum states of light created through such configurations, such as super-radiant states, can still offer advantages over the Shot-Noise Limit (SNL) [2]. In a super-radiant set up, a collection of excited atoms in a permutation-invariant subspace, decay photons into the port. This symmetry allows us to study the uncertainty of the phase estimation, using this light source. However, determining whether an arbitrary system of emitters possesses a quantum advantage remains nontrivial. For a general quantum state, the ultimate limit of error in parameter estimation can be addressed through the theory of Quantum Fisher Information (QFI) [3]. The noise limit for estimating the phase φ is constrained by the QFI of the quantum states $|\psi_\varphi\rangle$ utilized in metrology: $\delta\varphi \geq 1/(\sqrt{\mathrm{QFI}(|\psi\rangle_\varphi}))$, known as the Cramer-Rao Bound (CRB), where:

$$\mathrm{QFI}(|\psi\rangle_\varphi) = 4\left(\langle\dot{\psi}_\varphi|\dot{\psi}_\varphi\rangle - \left|\langle\dot{\psi}_\varphi|\psi_\varphi\rangle\right|^2\right). \tag{1.1}$$

Previously, the QFI has been calculated for simple cases where you have a single mode of light (such as NOON states) or some sort of symmetry within the system (such as super-radiant). Here, we present a comprehensive formula for the QFI of the quantum state of light, expressed in relation to the internal Hamiltonian of an arbitrary system of emitters that decay into optical ports and subsequently traverse a MZI setup to sense an unknown parameter φ. This connection enables the examination of the enhancement of the generated light state by exclusively studying the emitter system. However, the challenge in deriving the ultimate bound from the QFI lies in the necessity for an optimal measurement. In general, this measurement could extend beyond localities in both time and space, yet our access is confined to time-local photodetection at the output. We explore the optimal measurement and propose a protocol to attain the QFI bound. Additionally, we investigate the potential of the light sources in terms of the emitters' Hamiltonian.

Chapter 2

QUANTUM FISHER INFORMATION

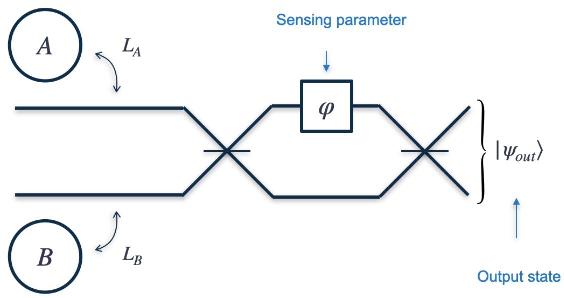

Figure 2.1: Schematic depiction of the light source model for the input of the MZI. In experiments, to prepare a general quantum state of light, a quantum system (e.g., atoms) emits photons into the light port. The sources interact with the ports through the jump operators L_A, and L_B.

In experiment, preparing an arbitrary photonic quantum state is not trivial. Typically, we have another quantum system (e.g. atoms), emitting photons into the optical port (Fig. 2.1). To address this, we examine a MZI where each arm initially exists in the vacuum state, coupled individually to the sources A and B. The emitter $X \in \{A, B\}$ resides in a D_X-dimensional Hilbert space, evolving with the Hamiltonian $H_X(t)$ (potentially time-dependent), emitting photons into a light port. We assume that the Hamiltonian $H_{I,X}(t)$ in the interaction picture, relative to the port's Hamiltonian, is given by:

$$H_{I,X}(t) = H_X(t) + (x_t L_X^\dagger + x_t^\dagger L_X). \tag{2.1}$$

Here, x_t represents the annihilation operator of the port in the time domain, and L_X is the jump operator of the system expressing the emitters' interaction with the port. This interaction model is Markovian [4], as the source interacts with a single mode x_t at each time step. This model can be applied to several experimental setups, such as in superconducting systems [5] and quantum dots [6]. If the source is initially in state $|\phi_{X,s}\rangle$ and the port is in a vacuum state, the state of the light channel after time T is expressed as:

$$|\psi_x\rangle = \frac{1}{C_X} \langle\phi_{X,f}| \mathcal{T}\exp\left(\int_0^T H_{I,X}(s)ds\right) |\phi_{X,s}, \mathrm{vac}\rangle\,, \tag{2.2}$$

where C_X is the normalization factor after projecting the source to the final state $|\phi_{X,f}\rangle$. The ports then pass through an MZI with the following unitary transformation for the annihilation operators:

$$U_{\mathrm{MZI}}^{\dagger} a_t U_{\mathrm{MZI}} = a_t \cos(\varphi) + b_t \sin(\varphi),$$
$$U_{\mathrm{MZI}}^{\dagger} b_t U_{\mathrm{MZI}} = b_t \cos(\varphi) - a_t \sin(\varphi).$$

Consequently, the final output state is given by:

$$|\psi_{a,b}(\varphi)\rangle = U_{\mathrm{MZI}} \left(|\psi_a\rangle \otimes |\psi_b\rangle\right). \tag{2.3}$$

We can compute the QFI for the described quantum state in relation to the channels $\mathcal{E}_X$, which characterize the evolution of the source $X \in \{A, B\}$.

$$\mathcal{E}_X(t,s) = \mathcal{T} \exp\left(\int_0^s \mathcal{L}_X(s')ds'\right), \tag{2.4}$$

where:

$$\mathcal{L}_X(t)\rho = -i[H_X(t), \rho] + L_X \rho L_X^{\dagger} - \frac{1}{2}\{L_X L_X^{\dagger}, \rho\}.$$

This computation allows us to assess its capability for parameter sensing concerning φ.

Proposition 1.— In the presented light model, particularly in the scenario of identical sources, the QFI at $\varphi = 0$ can be exclusively computed using the source Lindbladians:

$$\begin{aligned}\mathrm{QFI} = \frac{4}{C^2}\int_0^T\int_0^t \Bigg\{ &\left| \langle\phi_{X,f}|\, \mathcal{E}_X(T,t)\Big(\mathcal{E}_X(t,t')\big[L_X \mathcal{E}_X(t',0)(|\phi_{X,s}\rangle\langle\phi_{X,s}|)\big] L_X^{\dagger}\Big)\, |\phi_{X,f}\rangle \right|^2 \\ &- \left| \langle\phi_{X,f}|\, \mathcal{E}_X(T,t)\Big(L_X \mathcal{E}_X(t,t')\big[L_X \mathcal{E}_X(t',0)(|\phi_{X,s}\rangle\langle\phi_{X,s}|)\big]\Big)\, |\phi_{X,f}\rangle \right|^2 \Bigg\} dt dt' \\ + \frac{2}{C}\int_0^T \langle\phi_{X,f}|\mathcal{E}_X(T,t)\Big(L_X \mathcal{E}_X(t,0)(|\phi_{X,s}\rangle\langle\phi_{X,s}|) L_X^{\dagger}\Big)\, &|\phi_{X,f}\rangle\, dt.\end{aligned} \tag{2.5}$$

where,

$$C = \langle\phi_{X,f}|\, \mathcal{E}_X(T,0)(|\phi_{X,s}\rangle\langle\phi_{X,s}|)\, |\phi_{X,f}\rangle.$$

Proof sketch for Proposition 1.— By discretizing time into small bins of ϵ, the port can be treated as a collection of qubits in either the vacuum or the one-photon state $|1\rangle = \mathbf{X}_k |\mathrm{vac}\rangle$, where $k \in 1, \cdots, T/\epsilon$ is the qubit number, and:

$$\mathbf{X}_k = \frac{1}{\sqrt{\epsilon}}\int_{k\epsilon}^{(k+1)\epsilon} x_t dt,$$

and,

$$[\mathbf{X}_k, \mathbf{X}_l^{\dagger}] = \delta_{kl}.$$

Using this representation, the state of the light can be expressed as a Matrix Product State. Then we can compute the terms in the Eq.[1.1] and the take the limit of $\epsilon \to 0$, as shown in the appendix A. It is worth highlighting that the computation of the QFI from Eq. [2.5] takes place in a D-dimensional space of the source Hilbert space instead of the infinite dimensional space of the output photonic state. In cases where D does not scale with the number of photons emitted into the light channels, it can be efficiently computed. This formula allows for an examination to determine whether sensing with this specific light source in the experiment is beneficial and whether a quantum enhancement is achievable.

In a super-radiant setup, the number of photons scales with the number of atoms in the experiment. Therefore, to increase the number of photons in the optical port and achieve a smaller uncertainty in φ, one needs to increase the number of excited atoms. However, it is possible to prepare a photonic state with an arbitrary number of photons using only a small number of atoms. Consider a single atom excited by a laser: the atom can emit photons into the port and then be re-excited by the laser. In this scenario, the number of emitted photons is proportional to the duration the laser is on. Thus, we study the scaling of the QFI with the interaction time T. This allows us to determine whether a quantum advantage can be achieved using an emitter with a fixed-dimensional Hilbert space.

Corollary 1.— In the case of light sources where the Lindbladian $\mathcal{L}_X$ is primitive and has a single fixed point, the QFI is, at most, linearly proportional to the interaction time T.

By primitive we mean that the Lindbladian has no purely imaginary eigenvalues. Therefore, any state will evolve to the fixed point.

Proof sketch for Corollary 1.— The quadratic dependence on time T may arise from the double integral in Eq. [2.5]. When a single fixed point is present, the integrand displays exponential decay (shown in appendix B.1). Consequently, this term does not contribute a quadratic term in T.

Corollary 2.— In the case of light sources where the Lindbladian $\mathcal{L}_X$ is primitive and has two fixed points, the QFI can scale quadratically with respect to the interaction time T.

Proof sketch for Corollary 2.—We illustrate this with a simple example where the Hamiltonian $H_X = 0$, and the jump operator is:

$$L_X = \begin{pmatrix} 1 & 0 \\ 0 & e^{i\gamma} \end{pmatrix},$$

where γ is a constant phase. It is easy to see that both $|0\rangle$, and $|1\rangle$ are the fixed points. As shown in the appendix B.2, the QFI in this scenario scales as $\sin^2(\gamma)T^2$. Starting from a superposition state such as $\big(|0\rangle + |1\rangle\big)/\sqrt{2}$ in the emitter, the photonic state of the MZI input using this jump operator is a superposition of coherent states, i.e. $\big(|\alpha\rangle + |\alpha e^{i\gamma}\rangle\big)/\sqrt{2(1+\mathrm{Re}(\langle\alpha|\alpha e^{i\gamma}\rangle))}$. For cat states, it has been previously shown that they can result in a quantum-enhanced sensing [7] and in this illustrative example, we have shown that it can be experimentally accessible having an emitter with a Lindbladian of two fixed points.

Chapter 3

OPTIMAL MEASUREMENT

As previously mentioned, to achieve the precision determined by the QFI, we need to apply an optimal measurement on the output state. Generally, this measurement can be more complex than just photodetection and therefore, detection of photons in the output is not sufficient. In the next result, we introduce a method to achieve the CRB.

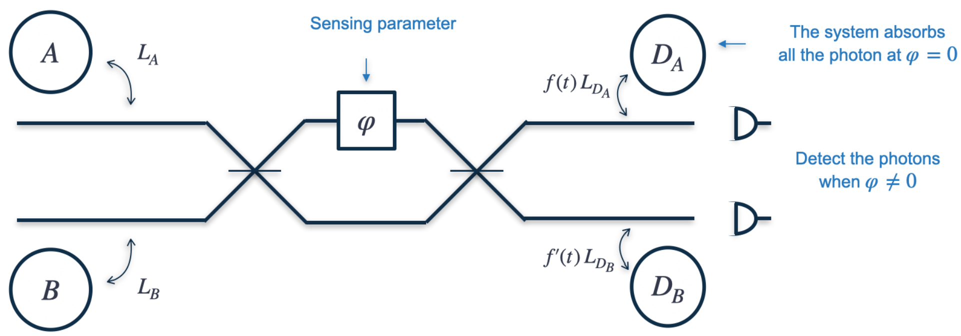

Figure 3.1: Schematic depiction of the optimal measurement. The auxiliary systems D_A and D_B are designed to absorb all the photons when $\varphi = 0$. When a non-zero phase exists, fluctuations occur in the optical port, allowing the detector to detect photons. In this case, photodetection combined with measurements on the auxiliary systems constitutes the optimal measurement for saturating the Cramér-Rao bound (CRB).

Proposition 2.— The ultimate QFI bound in Eq. [2.5] can be achieved by employing a time reversal, reabsorbing the photons into an auxiliary controlable system of dimension $D+2$, and performing photodetection on the output port along with a computational basis measurement on the absorbed photons (Fig. 3.1).

Proof sketch for Proposition 2.— The measurements $M_0 = I - |\psi\rangle\langle\psi|$, and $M_1 = |\psi\rangle\langle\psi|$, saturate the Cramer-Rao bound for any state $|\psi\rangle$ (shown in appendix C). One way to apply this projection is to use another controllable system D_X with a controllable interaction with the port. If we can apply any unitary between the port and the system D_X, we can just apply the inverse of the unitaries of the emitter and port to absorb all the photons. To make it more experimentally accessible, as shown in the appendix D, we can utilize a Hamiltonian of the form:

$$H = f(t)\big(a_t^\dagger \sigma + \text{h.c.}\big),$$

to apply a swap operator between a photonic qubit in the descitized notation and a two-level system, with σ being the projection from the excited state to the ground state. If we can apply this swap gate to a two-level system, then we can just have an additional D-dimensional system to apply the inverse unitary. The purpose of the swap gate is to make the absorption more experimentally accessible. It reduces the full controllability of the port and the D-dimensional system to full controllability of a $D+2$-dimensional system and a restricted control between the port and two levels of the absorption system. Therefore, if we can apply the reabsorption and do photodetection along measurement on the system D_X, then we are applying the projection on $|\psi\rangle\langle\psi|$. Therefore, this measurement saturates the Cramér-Rao bound and is optimal.

We demonstrate the reabsorption process using a simple example of a single atom under laser excitation (Fig. 3.2).

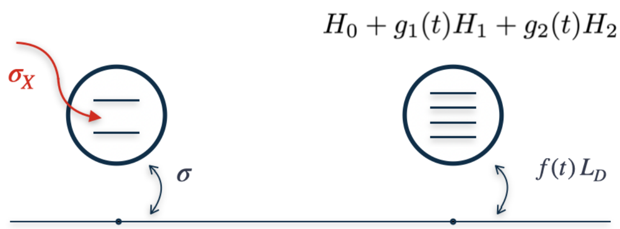

Figure 3.2: Figure showing the illustrative example to demonstrate the reabsoption. A 2-level system gets excited by a laser and emits photon into the port. The photons get reabsorbed into a controllable 4-level system. The control is over the interaction strenght $f(t)$, and the reabsorbption Hamiltonain terms by the coefficients $g_1(t)$ and $g_2(t)$.

We assume a 4-level system for reabsorption with the following Hamiltonian:

$$H(t) = H_0 + g_1(t)H_1 + g_2(t)H_2,$$

where H_0 is a diagonal Hamiltonian and H_1 and H_2 have non-zero elements only next to the diagonal. An example of full controllability of an absorption system with arbitrary dimension of Hilbert space is a Kerr nonlinear cavity [8]. In ref. [9], it is shown that this Hamiltonian can be universal. We also assume that the jump operator for the reabsorption system is $f(t)L_D$, where L_D is the projection from the first excited state to the ground state. The goal is to optimize $f(t)$, $g_1(t)$, and $g_2(t)$ such that the photon count at the output port is zero, ensuring that the auxiliary system absorbs all the photons. In Appendix E.1, we show that the emitter and reabsorption system can be considered as a single system interacting with the port, allowing us to express the number of photons in the output as a function of expectation values of operators in the joint system's Hilbert space. We consider the

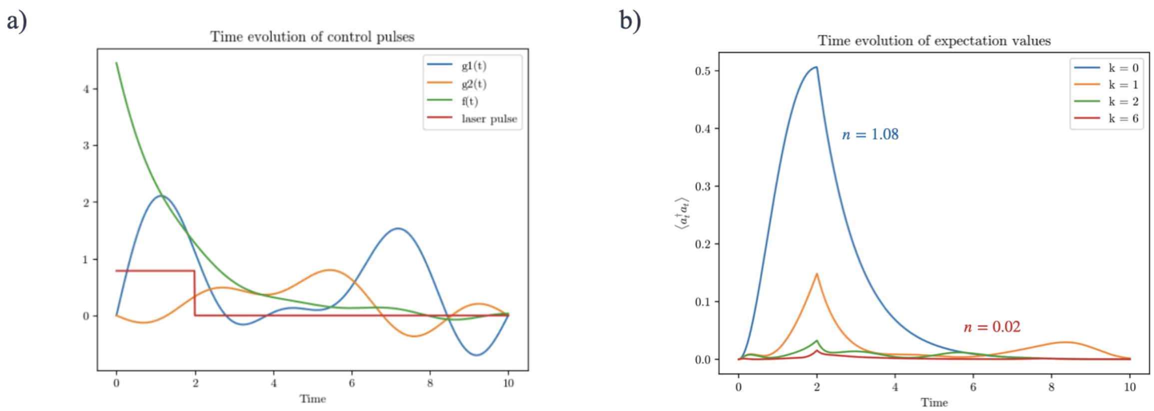

Figure 3.3: a) The optimized pulses for reabsorbing the photons as a function of time for $k_{\max} = 6$. The red line indicates when the laser is on the emitter. $f(t)$ is the interaction strength of the reabsorption system with the port, while $g_1(t)$ and $g_2(t)$ control the Hamiltonian of the 4-level system. b) The expectation value of $\langle a_t^\dagger a_t \rangle$ as a function of time for different values of $k_{\max}$. The area under each curve represents the total number of photons (n) in the output. $k = 0$ corresponds to the case where there is no reabsorption.

following ansatz for these pulses:

$$f(t), g_1(t), g_2(t) \sim \sum_{k=1}^{k_{\max}} \alpha_k \sin\left(\frac{2k\pi t}{T}\right) + \beta_k \cos\left(\frac{2k\pi t}{T}\right).$$

To optimize the αs and βs, we use the adjoint method as described in Appendix E.2 to find the gradient of the photon count with respect to the control pulses $f(t)$, $g_1(t)$, and $g_2(t)$. This allows us to minimize the photon count. The optimized results are shown in Fig. 3.3. The numerical simulations demonstrate that by controlling these pulses, we can absorb all the photons up to a desired error. Increasing the value of $k_{\max}$ reduces the error in reabsorption.

Although the absorption method for optimal measurement can be implemented in near term systems, we also study a simpler class of measurement, i.e. time-local photodetection with linear-optical elements and classical feedback (Fig. 3.4). We assume the linear element (Beam Splitter) to be controllable. Here there is no auxillary system for absorption and we only have access to apply photodetection and beam splitter with adjustable angle. The measurement is constructed as following: First, we detect a photon at time t_1 at either arms of the MZI output, a ($\sigma_1 = 0$) or b ($\sigma_1 = 1$). Based on the measurement outcome σ_1 and the detection time t_1, we change the angle of the controlable beam splitter on the output. Second we detect another photon at time t_2. Then we change the beam splitter angle based on σ_1,σ_2 and t_1,t_2. We continue this until all the photons are absorbed. This measurement after detection of n number of photons can be written as a projection on to the following state:

$$\left\langle E_{t_1,t_2,\cdots,t_n}^{\sigma_1,\sigma_2,\cdots,\sigma_n} \right| = \langle 0 | \left(f_{t_1,t_2,\cdots,t_n}^{\sigma_1,\sigma_2,\cdots,\sigma_n} a_{t_n} + g_{t_1,t_2,\cdots,t_n}^{\sigma_1,\sigma_2,\cdots,\sigma_n} b_{t_n} \right) \cdots \left(f_{t_1,t_2}^{\sigma_1,\sigma_2} a_{t_2} + g_{t_1,t_2}^{\sigma_1,\sigma_2} b_{t_2} \right) \left(f_{t_1}^{\sigma_1} a_{t_1} + g_{t_1}^{\sigma_1} b_{t_1} \right). \tag{3.1}$$

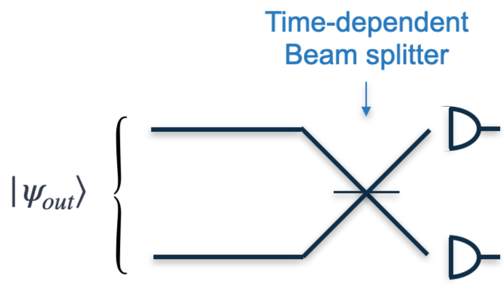

Figure 3.4: Figure indicating the linear-optical measurement. The angle of the beam splitter is controllable and can be adjusted based on classical feedback from the measurement outcome of the photodetection.

Proposition 3.— Photodetection alone is optimal if we ask: (1) the set of measurements in Eq.[3.1] for all $n \in \mathbb{N}$, be optimal and saturate the CRB, and (2) the two emitters A, and B be in a product state.
This means that if the two conditions are satisfied then all the coefficeints of f and g in Eq.[3.1] are either 0 or 1.

Proof sketch for Proposition 3.— In ref.[10], they show that LOCC (local operation and classical communication) measurement is optimal for any pure state, for a system of qubits. There, they use an operator M, defined as:

$$M = |\psi_\theta\rangle \langle\psi_\theta^\perp| - |\psi_\theta^\perp\rangle \langle\psi_\theta| \, ,$$

where $|\psi_\theta^\perp\rangle = (1 - |\psi_\theta\rangle \langle\psi_\theta|) \, d \, |\psi_\theta\rangle / d\theta$. The set of the measurements:

$$\{\langle E^{\sigma_1,\sigma_2,\cdots,\sigma_n}_{t_1,t_2,\cdots,t_n}| \, |\vec{\sigma} \in \{0,1\}^n, \vec{t} \in [0,T]^n, n \in \mathbb{N}\},$$

are optimal and saturates the CRB if they satisfy:

$$\langle E^{\sigma_1,\sigma_2,\cdots,\sigma_n}_{t_1,t_2,\cdots,t_n}| \, M \, |E^{\sigma_1,\sigma_2,\cdots,\sigma_n}_{t_1,t_2,\cdots,t_n}\rangle = 0.$$

By using these conditions and the fact that the emitters are in a product state, we show that the input photonic state of the MZI should satisfy a phase condition, which is fully described in the appendix F.1. Using this phase condition, we show that the basis for the f and g coefficients are either 0 or 1 to saturate the CRB. Therefore, photodetection is optimal, and there is no need for a linear element. However, in the appendix F.2, we construct an example in which an adjustable beam splitter can be beneficial when we have an entangled state initially in the two arms of the MZI. Therefore, for beam splitters to be effective for saturating the CRB, we need entanglement in the light source used for metrology. It is worth mentioning that this condition only studies the case when the measurement with linear optical elements saturates the CRB. There can be cases in which beam splitters are not useful for saturating the CRB, but a HL advantage can be achieved.

Chapter 4

CONCLUSION

In conclusion, we introduced an experimentally motivated protocol for quantum metrology. Using a Markovian model for the light source, we derive the resulting Quantum Fisher Information (QFI) of the photonic state after it passes through a Mach-Zehnder Interferometer (MZI) to measure an unknown parameter φ, indicating the best attainable uncertainty.

Next, we study scenarios where quantum advantage might be achieved. We demonstrate that using a quantum system to create states with an arbitrary number of photons, does not allow for quadratic quantum advantage if the Lindbladian is primitive and has a single fixed point. However, we show that if the system consists of two fixed points, there is potential for quantum advantage.

We then introduce the optimal measurement to achieve the best uncertainty given by the QFI in the Cramér-Rao bound (CRB). The optimal measurement is constructed by reabsorbing photons into an auxiliary controllable system and performing photodetection in the optical port. Finally, we study a simpler class of measurements, using linear-optical elements with classical feedback, and show that they can be effective to saturate CRB only if the two sources are initially entangled.

This study can help identify the experimental limitations in creating quantum states of light that provide a metrological advantage over the Standard Quantum Limit (SNL). Additionally, it provides a foundation for studying more complex photonic states to determine if they can offer quantum advantage.

BIBLIOGRAPHY

[1] Rafal Demkowicz-Dobrzański, Marcin Jarzyna, and Jan Kołodyński. Quantum limits in optical interferometry. *Progress in Optics*, 60:345–435, 2015.

[2] Vanessa Paulisch, Martí Perarnau-Llobet, Alejandro González-Tudela, and J Ignacio Cirac. Quantum metrology with one-dimensional superradiant photonic states. *Physical Review A*, 99(4):043807, 2019.

[3] Samuel L Braunstein and Carlton M Caves. Statistical distance and the geometry of quantum states. *Physical Review Letters*, 72(22):3439, 1994.

[4] Shanshan Xu and Shanhui Fan. Input-output formalism for few-photon transport: A systematic treatment beyond two photons. *Physical Review A*, 91(4):043845, 2015.

[5] Alexandre Blais, Arne L Grimsmo, Steven M Girvin, and Andreas Wallraff. Circuit quantum electrodynamics. *Reviews of Modern Physics*, 93(2):025005, 2021.

[6] AV Akimov, A Mukherjee, CL Yu, DE Chang, AS Zibrov, PR Hemmer, H Park, and MD Lukin. Generation of single optical plasmons in metallic nanowires coupled to quantum dots. *Nature*, 450(7168):402–406, 2007.

[7] Jaewoo Joo, William J Munro, and Timothy P Spiller. Quantum metrology with entangled coherent states. *Physical review letters*, 107(8):083601, 2011.

[8] Ming Yuan, Alireza Seif, Andrew Lingenfelter, David I Schuster, Aashish A Clerk, and Liang Jiang. Universal control in bosonic systems with weak kerr nonlinearities. *arXiv preprint arXiv:2312.15783*, 2023.

[9] Sonia G Schirmer, H Fu, and Allan I Solomon. Complete controllability of quantum systems. *Physical Review A*, 63(6):063410, 2001.

[10] Sisi Zhou, Chang-Ling Zou, and Liang Jiang. Saturating the quantum cramér–rao bound using locc. *Quantum Science and Technology*, 5(2):025005, 2020.

[11] Joshua Combes, Joseph Kerckhoff, and Mohan Sarovar. The slh framework for modeling quantum input-output networks. *Advances in Physics: X*, 2(3):784–888, 2017.

Appendix A

QUANTUM FISCHER INFORMATION OF THE LIGHT SOURCE

We present the calculation of Fischer information from a general light source emitting into a markovian channel. We will formulate the analysis of light source in the collision model picture, which will provide a clean description of the entire state of emitted photons. We consider a system described with time-dependent Hamiltonian $H_X(t)$, emitting into an output channel, described by buckets X_k, and additional dephasing channels described by buckets $X_{\alpha,k}$. Throughout, we use the time coarse-graining parameter ε, which is set to 0 to take the continuum limit that describes the actual experiment. Assuming the initial state of the system is $|\phi_{X,s}\rangle$, with no photons in the output port, the state after time $T = N\varepsilon$ is given by

$$|\psi_x\rangle = \frac{1}{C_X} \langle\phi_{X,f}|\, U_{X,N}U_{X,N-1}\dots U_{X,1}\,|\phi_{X,s},\text{vac}\rangle\,,$$

where

$$U_{X,k} = \exp\left[-i\Big(H_X(k\varepsilon)\varepsilon + \sqrt{\varepsilon}O_{X,k}\Big)\right] \text{ where } O_{X,k} = \big(X_k^\dagger L_X + \text{h.c.}\big) + \sum_\alpha \big(X_{\alpha,k}^\dagger L_{X,\alpha} + \text{h.c.}\big),$$

and

$$X_k = \frac{1}{\sqrt{\varepsilon}}\int_{k\varepsilon}^{(k+1)\varepsilon} x_t dt, \quad \Big[X_k, X_l^\dagger\Big] = \delta_{kl}.$$

and $|\phi_{X,f}\rangle$ is the final state of the system that we project into, C_X is the normalization factor, and $L_X, L_{X,\alpha}$ are the jump operators.

Now, we consider the standard interferometric setup where we have two sources, S_A and S_B, which emit into channels with bin operators a_t and b_t respectively, as well as additional decay channels $a_{\alpha,t}$ and $b_{\alpha,t}$ respectively. The bin operators a_t and b_t then are passed through a MZI interferometer with phase φ, which implements the transformation $(a_t, b_t) \to (a_t(\varphi), b_t(\varphi))$ as

$$a_t(\varphi) = U_{\text{MZI}}(\varphi)a_tU_{\text{MZI}}^\dagger(\varphi) = a_t\cos\varphi + b_t\sin\varphi. \tag{A.1a}$$

$$b_t(\varphi) = U_{\text{MZI}}(\varphi)b_tU_{\text{MZI}}^\dagger(\varphi) = b_t\cos\varphi - a_t\sin\varphi. \tag{A.1b}$$

It is convenient to note that

$$\frac{d}{d\varphi}a_t(\varphi) = b_t(\varphi) \text{ and } \frac{d}{d\varphi}b_t(\varphi) = -a_t(\varphi).$$

It's straightforward to see that the same relations hold for $(A_k, B_k) \to (A_k(\varphi), B_k(\varphi))$. We will now consider the state obtained after the MZI

$$|\psi(\varphi)\rangle = U_{\text{MZI}}(\varphi)\,|\psi_a\rangle \otimes |\psi_b\rangle = \frac{1}{C}\langle\phi_{A,f},\phi_{B,f}|\, U_{\text{MZI}}(\varphi)U_NU_{N-1}\dots U_1\,|\phi_{A,s},\phi_{B,s},0\rangle\,,$$

where $C = C_A C_B$, and we introduce $U_k = U_{A,k}U_{B,k}$. We can rewrite this state as

$$|\psi(\varphi)\rangle = \frac{1}{C}\langle\phi_{A,f},\phi_{B,f}|\, V_N V_{N-1}\dots V_1\,|\phi_{S_A},\phi_{S_B},0\rangle\,,$$

where $V_k = V_{A,k}V_{B,k}$ with

$$V_{X,k} = \exp\left[-i\Big(H_X(k\varepsilon)\varepsilon + \sqrt{\varepsilon}O_{X,k}(\varphi)\Big)\right] \text{ with } O_{X,k}(\varphi) = X_k^\dagger(\varphi)L_X + \sum_\alpha X_{\alpha,k}^\dagger L_{X,\alpha} + \text{h.c.}.$$

We now calculate the Fischer information for the output state.

$$\mathrm{FI}_{|\psi(\varphi)\rangle} = \left\|\frac{d}{d\varphi}|\psi(\varphi)\rangle\right\|^2 - \left|\langle\psi(\varphi)|\,\frac{d}{d\varphi}|\psi(\varphi)\rangle\right|^2$$

For this computation, it is convenient to have the following two results:

Result 1: For any operator in the Hilbert space of the sources A and B, Ω, we have

$$\langle 0|\, V_k^\dagger \Omega \frac{d}{d\varphi}V_k\,|0\rangle = \varepsilon(L_B^\dagger \Omega L_A - L_A^\dagger \Omega L_B) + O(\varepsilon^{3/2}).$$

Proof: We begin by writing

$$\langle 0|\, V_k^\dagger \Omega \frac{d}{d\varphi}V_k\,|0\rangle = \langle 0|\, V_{B,k}^\dagger V_{A,k}^\dagger \Omega \frac{d}{d\varphi}V_{A,k}V_{B,k}\,|0\rangle + \langle 0|\, V_{B,k}^\dagger V_{A,k}^\dagger \Omega V_{A,k}\frac{d}{d\varphi}V_{B,k}\,|0\rangle$$

We can also write

$$\frac{d}{d\varphi}V_{A,k} = -i\sqrt{\varepsilon}\big(B_k(\varphi)L_A^\dagger + B_k^\dagger(\varphi)L_A\big) - \frac{\varepsilon}{2}\{B_k(\varphi)L_A^\dagger + B_k^\dagger(\varphi)L_A, O_{A,k}(\varphi)\} + O(\varepsilon^{3/2}), \tag{A.2a}$$

$$\frac{d}{d\varphi}V_{B,i} = i\sqrt{\varepsilon}\big(A_k(\varphi)L_B^\dagger + A_k^\dagger(\varphi)L_B\big) + \frac{\varepsilon}{2}\{A_k(\varphi)L_B^\dagger + A_k^\dagger(\varphi)L_B, O_{B,k}(\varphi)\} + O(\varepsilon^{3/2}). \tag{A.2b}$$

Now, using these expressions we have

$$\begin{aligned}&\langle 0|\, V_{B,k}^\dagger V_{A,k}^\dagger \Omega \frac{d}{d\varphi}V_{A,k}V_{B,k}\,|0\rangle \\ &= -i\sqrt{\varepsilon}\,\langle 0|\,\big(I + i\sqrt{\varepsilon}O_{A,k} + i\sqrt{\varepsilon}O_{B,k}\big)\Omega B_k^\dagger(\varphi)L_A\,|0\rangle - i\sqrt{\varepsilon}\,\langle 0|\,\Omega B_k(\varphi)L_A^\dagger(I - i\sqrt{\varepsilon}O_{B,k})\,|0\rangle + O(\varepsilon^{3/2}) \\ &= \varepsilon\big(L_B^\dagger \Omega L_A - \Omega L_A^\dagger L_B\big) + O(\varepsilon^{3/2}).\end{aligned}$$

and

$$\begin{aligned}&\langle 0|\, V_{B,k}^\dagger V_{A,k}^\dagger \Omega V_{A,k}\frac{d}{d\varphi}V_{B,k}\,|0\rangle \\ &= i\sqrt{\varepsilon}\,\langle 0|\,(i\sqrt{\varepsilon}O_{A,k} + i\sqrt{\varepsilon}O_{B,k})\Omega B_k^\dagger(\varphi)L_B\,|0\rangle + i\sqrt{\varepsilon}\,\langle 0|\,\Omega(-i\sqrt{\varepsilon}O_{A,k}B_k^\dagger(\varphi)L_B)\,|0\rangle \\ &= \varepsilon(-L_A^\dagger \Omega L_B + \Omega L_A^\dagger L_B) + O(\varepsilon^{3/2}).\end{aligned}$$

Result 2: For any operator Ω in the Hilbert space of the sources A and B, we have

$$\langle 0|\, V_k^\dagger \Omega V_k\,|0\rangle = e^{\varepsilon\mathcal{L}_k^\dagger}(\Omega) + O(\varepsilon^2),$$

where $\mathcal{L}_k = \mathcal{L}_{A,k} + \mathcal{L}_{B,k}$,

$$\mathcal{L}_{X,k}(\Omega) = -i[\Omega, H_X(k\varepsilon)] + L_X \Omega L_X^\dagger - \frac{1}{2}\{L_X^\dagger L_X, \Omega\} + \sum_\alpha \bigg(L_{X,\alpha}\Omega L_{X,\alpha}^\dagger - \frac{1}{2}\{\Omega, L_{X,\alpha}^\dagger L_{X,\alpha}\}\bigg).$$

Proof: Follows just by Taylor expansion of $V_{A,k}$ and $V_{B,k}$.

Result 3: For any operator Ω in the Hilbert space of the sources A and B, we have

$$\langle 0| \frac{\mathrm{d}V_k^\dagger}{\mathrm{d}\varphi}\Omega\frac{\mathrm{d}V_k}{\mathrm{d}\varphi}|0\rangle = \epsilon\big(L_A^\dagger \Omega L_A + L_B^\dagger \Omega L_B\big) + O(\varepsilon^{3/2}),$$

Proof: Follows just by Taylor expansion of $V_{A,k}$ and $V_{B,k}$.

We now compute $d|\psi(\varphi)\rangle/d\varphi$. This can be written as

$$\frac{d|\psi(\varphi)\rangle}{d\varphi} = \frac{1}{C}\langle\phi_{A,f},\phi_{B,f}|\sum_{k=1}^{N} V_N V_{N-1}\dots V_{k+1}\frac{d}{d\varphi}V_k V_{k-1}\dots V_1|\phi_{A,s},\phi_{B,s},0\rangle.$$

defining

$$\rho_f = \rho_{A,f}\otimes\rho_{B,f} = |\phi_{A,f},\phi_{B,f}\rangle\!\langle\phi_{A,f},\phi_{B,f}|,$$

$$\rho_s = \rho_{A,s}\otimes\rho_{B,s} = |\phi_{A,s},\phi_{B,s}\rangle\!\langle\phi_{A,s},\phi_{B,s}|,$$

we can write

$$\begin{aligned}
&\langle\psi(\varphi)|\frac{d}{d\varphi}|\psi(\varphi)\rangle \\
&= \frac{1}{C^2}\sum_{k=1}^{N}\langle\phi_{A,s},\phi_{B,s},0|V_1^\dagger V_2^\dagger\dots V_k^\dagger\big(V_{k+1}^\dagger\dots V_N^\dagger(\rho_f)V_N\dots V_{k+1}\big)\frac{d}{d\varphi}V_k V_{k-1}\dots V_1|\phi_{A,s},\phi_{B,s},0\rangle, \\
&= \frac{1}{C^2}\varepsilon\sum_{k=1}^{N}\langle\phi_{A,s},\phi_{B,s}|e^{\mathcal{L}_1^\dagger\varepsilon}\big(e^{\mathcal{L}_2^\dagger\varepsilon}\dots\big(e^{\mathcal{L}_k^\dagger\varepsilon}(L_B^\dagger\circ L_A - L_A^\dagger\circ L_B)(e^{\mathcal{L}_{k+1}^\dagger\varepsilon}\dots e^{\mathcal{L}_N^\dagger\varepsilon}\rho_f)))|\phi_{A,s},\phi_{B,s}\rangle + O(N\varepsilon^{1.5}).
\end{aligned}$$

where

$$(L_A\circ L_B)\Omega = L_A\Omega L_B.$$

Now, we take the continuum limit — setting $N = T/\varepsilon$, where T is the total time for which the source has emitted photons and taking $\varepsilon\to 0$, we obtain that

$$\langle\psi(\varphi)|\frac{d}{d\varphi}|\psi(\varphi)\rangle = \frac{1}{C^2}\int_0^T \mathrm{Tr}\Big[\rho_f\mathcal{E}(T,t)(L_B^\dagger\circ L_A - L_A^\dagger\circ L_B)\mathcal{E}(t,0)(\rho_s)\Big]dt.$$

where

$$\mathcal{E}(t,s) = \mathcal{E}_A(t,s)\otimes\mathcal{E}_B(t,s), \quad \mathcal{E}_X(t,s) = \mathcal{T}\exp\bigg(\int_s^t \mathcal{L}_X(s')ds'\bigg).$$

We also note that if the two sources are identical, then

$$\langle\psi(\varphi)|\frac{d}{d\varphi}|\psi(\varphi)\rangle = 0.$$

Next, consider $\|d\,|\psi(\varphi)\rangle/d\varphi\|^2$. Note that in the manipulations below, we use $\prod$ as an ordered product i.e. $\prod_{i=1}^{N} M_i = M_1 M_2 \dots M_N$ and $\prod_{i=N}^{1} M_i = M_N M_{N-1} \dots M_1$. We begin by writing

$$\left\|\frac{d}{d\varphi}\,|\psi(\varphi)\rangle\right\|^2 = \sum_{k,l=1}^{N} \underbrace{\langle\phi_{A,s},\phi_{B,s},0|\left(\prod_{m=1}^{l-1} V_m\right)\left(\frac{d}{d\varphi}V_l^\dagger\right)\left(\prod_{m=l+1}^{N} V_m^\dagger\right)\frac{\rho_f}{C^2}\left(\prod_{m=N}^{k+1} V_m\right)\left(\frac{d}{d\varphi}V_k\right)\left(\prod_{m=k-1}^{1} V_m\right)|\phi_{A,s},\phi_{B,s},0\rangle}_{\mathcal{D}_{k,l}}.$$

Let us define

$$\mathcal{D}_> = \sum_{1\le k<l\le T}\mathcal{D}_{k,l}, \mathcal{D}_< = \sum_{1\le l<k\le T}\mathcal{D}_{k,l} \text{ and } \mathcal{D}_= = \sum_{1\le k\le T}\mathcal{D}_{k,k}.$$

Now, it is easy to see that $\mathcal{D}_> = \mathcal{D}_<^*$. The computation done below correctly calculates $\mathcal{D}_> + \mathcal{D}_<^* = 2\mathrm{Re}(\mathcal{D}_>)$. We now evaluate $\mathcal{D}_=$.

$$\mathcal{D}_= = \frac{1}{C^2}\sum_{i=1}^{N}\langle\phi_s,0|\,V_1^\dagger\dots V_{k-1}^\dagger\left(\frac{d}{d\varphi}V_k^\dagger\right)\left(V_{k+1}^\dagger\dots V_N^\dagger\rho_f V_N\dots V_{k+1}\right)\left(\frac{d}{d\varphi}V_k\right)V_{k-1}\dots V_1\,|\phi_s,0\rangle\,.$$

where $|\phi_s\rangle = |\phi_{A,s},\phi_{B,s}\rangle$. So, we have that in the limit of $\varepsilon\to 0$ and $N\to\infty$,

$$\mathcal{D}_= = \frac{1}{C^2}\int_0^T \langle\phi_{A,s},\phi_{B,s}|\,\mathcal{E}^\dagger(t,0)(L_A^\dagger\circ L_A + L_B^\dagger\circ L_B)\Big(\mathcal{E}^\dagger(T,t)\rho_f\Big)\,|\phi_{A,s},\phi_{B,s}\rangle\,dt.$$

For identical and independent sources, we have that

$$\mathcal{D}_= = \frac{2}{C^2}\,\mathrm{Tr}\,\Big(\rho_{X,f}\mathcal{E}_X(t,0)(\rho_{X,s})\Big)\int_0^T \mathrm{Tr}\,\Big(\rho_{X,f}\mathcal{E}_X(T,t)\big(L_X\mathcal{E}_X(t,0)(\rho_{X,s})L_X^\dagger\big)\Big)dt.$$

Next, we need to compute

$$\begin{aligned}
2\mathrm{Re}(\mathcal{D}_>) &= \frac{2}{C^2}\mathrm{Re}\Bigg[\sum_{1\le k<l\le N}\langle\phi_s,0|\,V_1^\dagger V_2^\dagger\dots V_{l-1}^\dagger\left(\frac{d}{d\varphi}V_l^\dagger\right)\Big(\mathcal{E}_{l+1,N}^\dagger(\rho_f)\Big)V_l V_{l-1}\dots V_{k+1}\left(\frac{d}{d\varphi}V_k\right)V_{k-1}\dots V_1\,|\phi_s,0\rangle\Bigg],\\
&= \frac{2\varepsilon}{C^2}\mathrm{Re}\Bigg[\sum_{1\le k<l\le N}\langle\phi_s,0|\,V_1^\dagger\dots V_{l-1}^\dagger(L_A^\dagger\circ L_B - L_B^\dagger\circ L_A)\Big(\mathcal{E}_{l+1,N}^\dagger(\rho_f)\Big)V_{l-1}\dots V_{k+1}\left(\frac{d}{d\varphi}V_k\right)V_{k-1}\dots V_1\,|\phi_s,0\rangle\Bigg],\\
&= \frac{2\varepsilon}{C^2}\mathrm{Re}\Bigg[\sum_{1\le k<l\le N}\langle\phi_s,0|\,V_1^\dagger\dots V_k^\dagger\mathcal{E}_{k+1,l-1}^\dagger\Big(L_A^\dagger\circ L_B - L_B^\dagger\circ L_A\Big)\Big(\mathcal{E}_{l+1,N}^\dagger(\rho_f)\Big)\left(\frac{d}{d\varphi}V_k\right)V_{k-1}\dots V_1\,|\phi_s,0\rangle\Bigg]\\
&= \frac{2\varepsilon^2}{C^2}\mathrm{Re}\Bigg[\sum_{1\le k<l\le T}\langle\phi_s,0|\,V_1^\dagger\dots V_{k-1}^\dagger\Big(L_B^\dagger\circ L_A - L_A^\dagger\circ L_B\Big)\mathcal{E}_{k+1,l-1}^\dagger\Big(L_A^\dagger\circ L_B - L_B^\dagger\circ L_A\Big)\Big(\mathcal{E}_{l+1,N}^\dagger(\rho_f)\Big)V_{k-1}\dots V_1\,|\phi_s,0\rangle\Bigg],\\
&= \frac{2\varepsilon^2}{C^2}\mathrm{Re}\Bigg[\sum_{1\le k<l\le N}\langle\phi_s|\,\mathcal{E}_{1,k-1}^\dagger\Big(L_B^\dagger\circ L_A - L_A^\dagger\circ L_B\Big)\mathcal{E}_{k+1,l-1}^\dagger\Big(L_A^\dagger\circ L_B - L_B^\dagger\circ L_A\Big)\Big(\mathcal{E}_{l+1,N}^\dagger(\rho_f)\Big)\,|\phi_s\rangle\Bigg]
\end{aligned}$$

where we have defined, for $p\le q$,

$$\mathcal{E}_{p,q}(X) = e^{\mathcal{L}_q\varepsilon}\Big(e^{\mathcal{L}_{q-1}^\dagger\varepsilon}\dots\Big(e^{\mathcal{L}_p^\dagger\varepsilon}(X)\Big)\Big)$$

We can now pass into the continuum limit and setting the two sources to be identical,

$$2\mathrm{Re}(\mathcal{D}_<) = \frac{4}{C^2}\int_0^T\int_0^t \Bigg\{ \bigg|\mathrm{Tr}\left(\rho_{X,f}\mathcal{E}_X^\dagger(T,t)\big(\mathcal{E}_X^\dagger(t,t')\big[L_X\mathcal{E}_X^\dagger(t',0)(\rho_{X,s})\big]L_X^\dagger\big)\right)\bigg|^2 \tag{A.3}$$

$$-\bigg|\mathrm{Tr}\left(\rho_{X,f}\mathcal{E}_X^\dagger(T,t)\big(L_X\mathcal{E}_X^\dagger(t,t')\big[L_X\mathcal{E}_X^\dagger(t',0)(\rho_{X,s})\big]\big)\right)\bigg|^2\Bigg\}dtdt'. \tag{A.4}$$

Combining these expressions, we have that,

$$\left\|\frac{d}{d\varphi}\left|\psi(\varphi)\right\rangle\right\|^2 = \frac{4}{C^2}\int_0^T\int_0^t \Bigg\{ \bigg|\mathrm{Tr}\left(\rho_{X,f}\mathcal{E}_X(T,t)\big(\mathcal{E}_X(t,t')\big[L_X\mathcal{E}_X(t',0)(\rho_{X,s})\big]L_X^\dagger\big)\right)\bigg|^2$$
$$-\bigg|\mathrm{Tr}\left(\rho_{X,f}\mathcal{E}_X(T,t)\big(L_X\mathcal{E}_X(t,t')\big[L_X\mathcal{E}_X(t',0)(\rho_{X,s})\big]\big)\right)\bigg|^2\Bigg\}dtdt'$$
$$+\frac{2}{C}\int_0^T \mathrm{Tr}\left(\rho_{X,f}\mathcal{E}_X(T,t)\big(L_X\mathcal{E}_X(t,0)(\rho_{X,s})L_X^\dagger\big)\right)dt.$$

where:

$$C = \mathrm{Tr}\left(\rho_{X,f}\mathcal{E}_X(T,0)(\rho_{X,s})\right).$$

Appendix B

QUANTUM FISHER INFORMATION SCALING WITH TIME

B.1 Single Fixed point

For a Lindbladian with a single fixed point σ, in which $\mathcal{L}(\sigma) = 0$, we can write

$$\mathcal{E}(t,s)\rho = \mathrm{tr}(\rho)\sigma + \mathcal{M}(t,s)\rho, \tag{B.1}$$

and,

$$\|\mathcal{M}(t,s)\|_\diamondsuit \leq ce^{-\kappa(t-s)},$$

where c, and κ are positive constants. For identical sources, the double integral term in Eq.[2.5], can be written as:

$$\mathrm{QFI}^{(2)} = \frac{4}{C^2}\int_0^T\int_0^t \left\{\left|\mathrm{Tr}\left(\rho_f\mathcal{E}(T,t)\Big(\mathcal{E}(t,t')\big[L\mathcal{E}(t',0)(\rho_s)\big]L^\dagger\Big)\right)\right|^2 - \left|\mathrm{Tr}\left(\rho_f\mathcal{E}(T,t)\Big(L\mathcal{E}(t,t')\big[L\mathcal{E}(t',0)(\rho_s)\big]\Big)\right)\right|^2\right\}dtdt'$$

By using the Eq.[B.1], we get the upper bound for the integral:

$$\mathrm{QFI}^{(2)} \leq 4\int_0^T\int_0^t \left(\left|\mathrm{tr}\left(L^\dagger\sigma\right)\mathrm{tr}\left(L\sigma\right)\right|^2 - \left|\mathrm{tr}\left(L\sigma\right)\mathrm{tr}\left(L\sigma\right)\right|^2 + c_1e^{-\alpha_1(T-t)} + c_2e^{-\alpha_2(t-t')} + c_3e^{-\alpha_3 t'}\right)dtdt' = O(T),$$

where we assumed $\mathrm{Tr}(\rho_f\sigma) \neq 0$, and we used the fact that σ is a valid density matrix and therefore $\left|\mathrm{tr}\big(L^\dagger\sigma\big)\right| = |\mathrm{tr}(L\sigma)|$. As a result, in case of the Lindbladian with a single fixed point, the scaling of the QFI is linear with the total time T.

B.2 Two Fixed point

Here, using an example, we show that for the case of a Lindbladian with two fixed point, the scaling of the QFI can be quadratic with time T. For a Lindbladian with two fixed points σ_1, and σ_2, we can write:

$$\mathcal{E}(t,s)\rho = \mathrm{tr}(P_1\rho)\sigma_1 + \mathrm{tr}(P_2\rho)\sigma_2 + \mathcal{M}(t,s)\rho, \tag{B.2}$$

where P_1, and P_2 are projections, and:

$$\|\mathcal{M}(t,s)\|_\diamondsuit \leq ce^{-\kappa(t-s)},$$

where c, and κ are positive constants. Now suppose a system with the Hamiltonian $H = 0$ and the jump operator L and fixed points as follows:

$$L = \begin{pmatrix} 1 & 0 \\ 0 & e^{i\gamma} \end{pmatrix}, \quad \sigma_1 = P_1 = \begin{pmatrix} 1 & 0 \\ 0 & 0 \end{pmatrix}, \quad \sigma_2 = P_2 = \begin{pmatrix} 0 & 0 \\ 0 & 1 \end{pmatrix}.$$

If the initial and final state of the system is $(|0\rangle + |1\rangle)/\sqrt{2}$, we have:

$$\mathrm{Tr}(\rho\sigma_1) = \mathrm{Tr}(\rho\sigma_2) = 1$$

Inserting this into the QFI, we get:

$$\mathrm{QFI}^{(2)} = 4\int_0^T \int_0^t \left(\left| \left(\alpha \,\mathrm{tr}\big(L^\dagger \sigma_1\big) + \beta \,\mathrm{tr}\big(L^\dagger \sigma_2\big) \right) \right|^2 - \left| \left(\alpha \,\mathrm{tr}(L\sigma_1) + \beta \,\mathrm{tr}(L\sigma_2) \right) \right|^2 \right) dtds + O(T),$$

and,

$$\alpha = \mathrm{tr}\left(P_1 L \sigma_1\right) \mathrm{tr}\left(P_1 \rho\right) + \mathrm{tr}\left(P_1 L \sigma_2\right) \mathrm{tr}\left(P_2 \rho\right),$$

$$\beta = \mathrm{tr}\left(P_2 L \sigma_1\right) \mathrm{tr}\left(P_1 \rho\right) + \mathrm{tr}\left(P_2 L \sigma_2\right) \mathrm{tr}\left(P_2 \rho\right).$$

then $\alpha = 1/2$, and $\beta = e^{i\gamma}/2$. Therefore:

$$\mathrm{QFI}^{(2)} = 4\int_0^T \int_0^t \sin^2(\gamma) dtds + O(T), \tag{B.3}$$

$$= 2\sin^2(\gamma) T^2 + O(T) = \Omega(T^2). \tag{B.4}$$

As a result, in the case of the Lindbladian with two fixed points, the QFI can scale quadratically with time T.

Appendix C

OPTIMAL MEASUREMENT FOR SATURATING THE CRAMER-RAO BOUND

Here we show that the measurements $M_0 = |\psi\rangle\langle\psi|$, and $M_1 = I - |\psi\rangle\langle\psi|$ saturate the Cramer-Rao Bound. The Classical Fischer Information resulting from the measurements M_0, M_1, can be written as:

$$\text{CFI} = \sum_i \frac{1}{P_i}\left(\frac{dP_i}{d\varphi}\right)^2,$$

where,

$$P_i = \langle\psi_\varphi|\, M_i\, |\psi_\varphi\rangle\,.$$

Next we compute the derivative of P_i with respect to φ:

$$\frac{dP_i}{d\varphi} = \langle\partial_\varphi\psi|\, M_i\, |\psi\rangle + \langle\psi|\, M_i\, |\partial_\varphi\psi\rangle\,,$$

since $P_0 = 1$, $dP_0/d\varphi = 0$, and $P_1 = 0$, $dP_1/d\varphi = 0$, we can write the CFI as:

$$\rightarrow \text{CFI} = 2\frac{d^2 P_1}{d\varphi^2}$$

$$\rightarrow \frac{d^2 P_1}{d\varphi^2} = 2\,\langle\partial_\varphi\psi|\, M_1\, |\partial_\varphi\psi\rangle + \langle\psi|\, M_1\, \left|\partial_\varphi^2\psi\right\rangle + \left\langle\partial_\varphi^2\psi\right|\, M_1\, |\psi\rangle = 2\,\langle\partial_\varphi\psi|\, M_1\, |\partial_\varphi\psi\rangle\,,$$

$$\implies \text{CFI} = 4\left(\left\|\left|\dot{\psi}\right\rangle\right\|^2 - \left|\left\langle\dot{\psi}\middle|\,\psi\right\rangle\right|^2\right) = \text{QFI}$$

Appendix D

ATOM-PORT INTERACTION FOR SWAP GATE IMPLEMENTATION

In this section we construct a model to perform a SWAP gate between an atom and a small bin of length ϵ in an optical port. Consider the Hamiltonian of the port and atom as following:

$$H = f(t)\big(a_t^\dagger \sigma + \text{h.c.}\big),$$

where $f(t)$ is the time-dependent interaction strength, a_t is the annihilation operator of the port in time domain, and σ is the projection of the excited state to the ground state of the atom. Writing the equation of motion for $a_\tau(t)$ in the Heisenberg picture:

$$\frac{\mathrm{d}a_\tau(t)}{\mathrm{d}t} = -if(t)\sigma(t)\delta(t-\tau),$$

$$\rightarrow a_\tau(t) = a_\tau(0) - i\int_0^t f(s)\sigma(s)\delta(s-\tau)ds,$$

$$\rightarrow a_\tau(t) = a_\tau(0) - i\begin{cases} t<\tau : 0, \\ t=\tau : \frac{f(\tau)\sigma(\tau)}{2}, \\ t>\tau : f(\tau)\sigma(\tau). \end{cases} = a_\tau(0) - if(\tau)\sigma(\tau)\theta(t,\tau).$$

Next we write the equation of motion for σ:

$$\frac{\mathrm{d}\sigma(t)}{\mathrm{d}t} = -if(t)a_t(t) = -if(t)\big(a_t(0) - i\frac{f(t)\sigma(t)}{2},$$
$$= -if(t)a_t(0) - \frac{f^2(t)}{2}\sigma(t).$$

Solving the above equation:

$$\sigma(t) = \sigma(0)e^{-\frac{1}{2}\int_0^t f(t')dt'} - i\int_0^t f(t')a_{t'}(0)e^{-\frac{1}{2}\int_{t'}^t f^2(s)ds}dt'.$$

For applying a swap operator, we need the excited state in a small time bin of ε, change to a excited state in the atom.

$$|\psi(0)\rangle = A_k|0\rangle = \frac{1}{\sqrt{\varepsilon}}\int_0^\varepsilon a_t^\dagger dt\,|0\rangle\,,$$

$$\rightarrow |\psi(\varepsilon)\rangle = \frac{1}{\sqrt{\varepsilon}}\int_0^\varepsilon a_t^\dagger(\varepsilon^-)dt\,|0\rangle\,.$$

Now, using the relation for $a_t(\varepsilon^-)$, we get:

$$\begin{aligned}|\psi(\varepsilon)\rangle &= \frac{1}{\sqrt{\varepsilon}}\int_0^\varepsilon \left(a_t^\dagger(0) + if(t)\left[\sigma^\dagger(0)e^{-\frac{1}{2}\int_0^t f^2(t')dt'} + i\int_0^t f(t')a_{t'}^\dagger(0)e^{-\frac{1}{2}\int_{t'}^t f^2(s)ds}dt'\right]\right)|0\rangle\, dt,\\ &= \frac{1}{\sqrt{\varepsilon}}\int_0^\varepsilon \left[a_t^\dagger(0) - f(t)\int_0^t f(t')a_{t'}^\dagger(0)e^{-\frac{1}{2}\int_{t'}^t f^2(s)ds}dt'\right]|0\rangle\, dt + \sigma^\dagger(0)\left(\frac{i}{\sqrt{\varepsilon}}\int_0^\varepsilon f(t)e^{-\frac{1}{2}\int_0^t f^2(s)ds}\right).\end{aligned}$$

Therefore, for $0 < \tau < \varepsilon$, the coefficient for $a_\tau^\dagger(0)$ is:

$$\langle 0|\, a_\tau(0)\, |\psi(\varepsilon)\rangle = 1 - \int_\tau^\varepsilon f(t)f(\tau)e^{-\frac{1}{2}\int_\tau^t f^2(s)ds}dt.$$

The function $f^2(t) = 1/(\varepsilon - t)$, makes the above equation to be zero and therefore, for applying a swap gate on a small bin of length ε, the interaction strength should be changed as:

$$f(t) = \frac{1}{\sqrt{\varepsilon - t}}.$$

Appendix E

OPTIMIZING REABSORPTION PULSES

E.1 SLH formalism + photon count formula

In the optimal measurement scenario, we assume a system S emits photons into the optical port and after the photonic state passes through the MZI interferometer, the photons get absorbed into another controlable system D. The system D is designed in such a way that it absorbs all the photons at MZI phase $\varphi = 0$. In this case the untiary for the MZI is identity and therefore we can see the whole system as S and D interacting with a single port. This allows us to use the SLH formalism [11] in which we can write the effective Hamiltonian and jump as:

$$H_{\text{eff}} = H_S + H_D - \frac{i}{2}(L_D^\dagger L_S - L_S^\dagger L_D),$$
$$L_{\text{eff}} = L_S + L_D,$$

where L_S and L_D are the individual jump operators of S and D. To find the control parameters for the system D, in order to absorb all the photon, we need to minimize the photon count at the optical port. Starting from the vacuum state in the port, we can write the output photon count as:

$$n = \int_{-0}^{T} \langle \phi, 0| \, a_t^\dagger(T^+) a_t(T^+) \, |\phi, 0\rangle \, dt = \sum_{k=0}^{N} \langle \phi, 0| \, U^\dagger(T^+, 0) A_k^\dagger A_k U(T^+, 0) \, |\phi, 0\rangle \, ,$$
$$= \sum_{k=0}^{N} \langle \phi, 0| \, U_1^\dagger \dots U_N^\dagger A_k^\dagger A_k U_N \dots U_1 \, |\phi, 0\rangle = \sum_{k=0}^{N} \langle \phi, 0| \, U_1^\dagger \dots U_k^\dagger A_k^\dagger A_k U_k \dots U_1 \, |\phi, 0\rangle \, .$$

where:

$$A_k = \frac{1}{\sqrt{\varepsilon}} \int_{k\varepsilon}^{(k+1)\varepsilon} a_t dt, \quad N\epsilon = T,$$
$$U_k = I - i\epsilon H(k\epsilon) - i\sqrt{\epsilon}\big(L^\dagger(k\epsilon) A_k + \text{h.c.}\big).$$

Therefore:

$$n = \sum_{k=0}^{N} \langle \phi, 0| \, U_1^\dagger \dots U_{k-1}^\dagger L^\dagger(k\epsilon) L(k\epsilon) U_{k-1} \dots U_1 \, |\phi, 0\rangle \, \epsilon = \int_0^T \langle \phi| \, \mathcal{E}^\dagger(t, 0) \Big(L^\dagger(t) L(t) \Big) \, |\phi\rangle \, dt.$$

where:

$$\mathcal{E}(t, 0) = \mathcal{T} e^{\int_0^t \mathcal{L}(s) ds}, \quad \mathcal{L}(t)\rho = -i[H, \rho] + L(t)\rho L^\dagger(t) - \frac{1}{2}\{L^\dagger(t) L(t), \rho\}.$$

Assuming system D to be controllable:

$$H = H_S + H_{D,0} + g(t) H_{D,1} - \frac{if(t)}{2}\big(L_D^\dagger L_S - L_S^\dagger L_D\big), \quad L(t) = L_S + f(t) L_D$$

where $H_{D,0}$ is diagonal and $H_{D,1}$ has terms like $|n\rangle\langle n+1|$, and $g(t)$ and $f(t)$ are real functions of time. Using this Hamiltonian, we need to find:

$$\langle L^\dagger(t)L(t)\rangle = \langle L_S^\dagger L_S\rangle + f^2(t)\langle L_D^\dagger L_D\rangle + f(t)\langle L_S^\dagger L_D + L_D^\dagger L_S\rangle.$$

and then compute the integral to find the photon counts at the output.

E.2 Adjoint method

To find the gradiant of the photon number (n) with respect to the control pulses we use the adjoint method. Consider the following ansatz for the functions $f(t)$ and $g(t)$:

$$g(t) = \sum_{k=1}^{k_{\max}} \alpha_k g_k(t) = \sum_{k=1}^{k_{\max}} \alpha_k \sin\left(k\frac{2\pi t}{T}\right), \quad f(t) = \sum_{k=1}^{k_{\max}} \beta_k f_k(t) = \sum_{k=1}^{k_{\max}} \beta_k \sin\left(k\frac{2\pi t}{T}\right).$$

which gives:

$$\frac{\mathrm{d}g(t)}{\mathrm{d}\alpha_k} = g_k(t), \quad \frac{\mathrm{d}f(t)}{\mathrm{d}\beta_k} = f_k(t).$$

for $p \in \{\alpha_k, \beta_k\}$, we can write:

$$\frac{\mathrm{d}n}{\mathrm{d}p} = \int_0^T \left(\mathrm{Tr}\left(O(t,p)\frac{\partial\rho(t,p)}{\partial p}\right) + \mathrm{Tr}\left(\frac{\partial O(t,p)}{\partial p}\rho(t,p)\right)\right)dt, \quad O(t,p) = L^\dagger(t)L(t).$$

We can write the second term as:

$$\mathrm{Tr}\left(\frac{\partial O(t)}{\partial p}\rho(t)\right) = 2f(t)f_k(t)\delta_{p,\beta_k}\langle L_D^\dagger L_D\rangle + f_k(t)\delta_{p,\beta_k}\langle L_S^\dagger L_D + L_D^\dagger L_S\rangle.$$

To compute the first term, we can write:

$$\rho(t) = \mathcal{E}(t,0)\rho(0), \quad \mathcal{E}(t,t') = \mathcal{T}e^{\int_{t'}^t \mathcal{L}(s)ds}.$$

Therefore,

$$\frac{\partial\rho(t,p)}{\partial p} = \int_0^t \mathcal{E}(t,t',p)\frac{\partial\mathcal{L}(t',p)}{\partial p}\rho(t',p)dt',$$

where we used $\partial\rho(0)/\partial p = 0$. By inserting this to the first term of $\mathrm{d}n/\mathrm{d}p$, we get:

$$\begin{aligned}\int_0^T \mathrm{Tr}\left(O(t,p)\frac{\partial\rho(t,p)}{\partial p}\right)dt &= \int_0^T dt\int_0^t dt'\,\mathrm{Tr}\left(O(t,p)\mathcal{E}(t,t',p)\frac{\partial\mathcal{L}(t',p)}{\partial p}\rho(t',p)\right)\\ &= \int_0^T dt'\int_{t'}^T dt\,\mathrm{Tr}\left(O(t,p)\mathcal{E}(t,t',p)\frac{\partial\mathcal{L}(t',p)}{\partial p}\rho(t',p)\right)\\ &= \int_0^T dt'\,\mathrm{Tr}\left(V(t')\frac{\partial\mathcal{L}(t',p)}{\partial p}\rho(t',p)\right)\end{aligned}$$

where:

$$V(t') = \int_{t'}^T \mathcal{E}^\dagger(t,t')O(t)dt.$$

To find $V(t')$ for all times we can solve the following differential equation:

$$\frac{\mathrm{d}V(t')}{\mathrm{d}t} = -O(t') - \mathcal{L}^\dagger(t')V(t'), \quad V(T) = 0$$

where:

$$\mathcal{L}^\dagger(t')\Omega = i[H, \Omega] + L^\dagger \Omega L - \frac{1}{2}\{L^\dagger L, \Omega\}.$$

Next we need to find the derivative of $\mathcal{L}$:

$$\frac{\partial \mathcal{L}(t', p)}{\partial p} = -i[\frac{\partial H}{\partial p}, \rho] + \frac{\partial L}{\partial p}\rho L^\dagger + L\rho\frac{\partial L^\dagger}{\partial p} - \frac{1}{2}\{\frac{\partial (L^\dagger L)}{\partial p}, \rho\}$$

inserting this, we need to find the expectation of the operator:

$$W(t') = i[\frac{\partial H}{\partial p}, V(t')] + \frac{\partial L^\dagger}{\partial p}V(t')L + L^\dagger V(t')\frac{\partial L}{\partial p} - \frac{1}{2}\{\frac{\partial (L^\dagger L)}{\partial p}, V(t')\}$$

Finally the derivative of n can be written as:

$$\frac{\mathrm{d}n}{\mathrm{d}p} = \int_0^T dt \langle W(t) + \frac{\partial (L^\dagger L)}{\partial p}\rangle.$$

with:

$$\frac{\partial H(t)}{\partial p} = g_k(t)\delta_{p,\alpha_k} H_{D,1} - f_k(t)\delta_{p,\beta_k}\frac{i}{2}(L_D^\dagger L_S - L_S^\dagger L_D),$$

$$\frac{\partial L(t)}{\partial p} = f_k(t)\delta_{p,\beta_k} L_D.$$

Appendix F

BEAM SPLITTERS + PHOTODETECTION OPTIMALITY

The optimality of a measurement is defined by the ability to extract the sensing parameter with the ultimate precision, known as the Cramer-Rao bound, from the measurement outcomes. In the context of an MZI setup, it has been demonstrated that photodetection (parity measurement) is the optimal method for achieving the Cramer-Rao bound when the quantum states utilized for metrology have a definite number of photons. However, this optimality does not hold in the general case, necessitating more intricate measurements. In reference [10], it has been established that, for pure states, a LOCC (Local Operations and Classical Communication) measurement can be identified as optimal. Here we study this optimality using linear-optical elements i.e. beam splitter with adjustable angle and photodetection. The full measurement protocol that we study is as follows: After detecting the first photon, the state undergoes controlled manipulation through a controllable beamsplitter. The parameters of this beamsplitter depend on the MZI arm of the initial photodetection and the time at which it occurred. Subsequently, upon detecting another photon, the angle of the beamsplitter is adjusted based on the measurement outcome. This adjustment is achieved through classical computation, utilizing the results obtained up to the current time. The process then repeats with the next photodetection. This can be regarded as a LOCC in which measurement results are employed iteratively to modify the beamsplitter parameters. In this section, we study the optimality condition of this type of measurement.

We will work directly in the continuum limit. The Hamiltonian for the MZI interferometer can be written as

$$H_\theta(t) = 2i \tan\frac{\theta}{2}\left(a_t^\dagger b_t - a_t b_t^\dagger\right).$$

It can be verified that the operator:

$$S_\theta = \lim_{\substack{t_+\to\infty \\ t_-\to-\infty}} \mathcal{T}\exp\left(-i\int_{t_-}^{t_+} H_\theta(s)ds\right),$$

transforms the operators a_t, and b_t as follows:

$$S_\theta^\dagger a_t S_\theta = a_t\cos\theta + b_t\sin\theta \quad \text{and} \quad S_\theta^\dagger b_t S_\theta = b_t\cos\theta - a_t\sin\theta.$$

Now, we consider $|\psi\rangle$ to be the initial wave function of the two ports. After passing through the MZI interferometer, the output wave function can be written as, $|\psi_\theta\rangle = S_\theta|\psi\rangle$. Using the first theorem from ref. [10], for any pure state $|\psi_\theta\rangle$, the set of measurement operators $\{|E_x\rangle\langle E_x|\}$, saturates the quantum cramer rao bound if and only if:

$$\langle E_x| M |E_x\rangle = 0 \quad \forall x, \tag{F.1}$$

and,

$$\forall x \,\text{s.t.}\ \langle E_x|\,\psi_\theta\rangle = 0, \quad \langle E_x|\,\psi_\theta^\perp\rangle = 0,$$

where,

$$M = |\psi_\theta\rangle\,\langle\psi_\theta^\perp| - |\psi_\theta^\perp\rangle\,\langle\psi_\theta| \quad \text{and} \quad |\psi_\theta^\perp\rangle = (1 - |\psi_\theta\rangle\,\langle\psi_\theta|)\,\frac{d\,|\psi_\theta\rangle}{d\theta}.$$

By taking the derivative of $|\psi_\theta\rangle$:

$$\frac{d\,|\psi_\theta\rangle}{d\theta} = -i\int_{-\infty}^{\infty}\frac{dH_\theta(s)}{d\theta}\,|\psi_\theta\rangle\,ds,$$

we can write the matrix M at $\theta = 0$:

$$iM = 2\,\langle\psi|\,H\,|\psi\rangle\,|\psi\rangle\,\langle\psi| - \big(\,|\psi\rangle\,\langle\psi|\,H + H\,|\psi\rangle\,\langle\psi|\,\big),$$

where we defined $H = i\int_{-\infty}^{\infty}\big(a_t^\dagger b_t - a_t b_t^\dagger\big)dt$. In the second theorem of ref. [10], it is demonstrated that for a wave function $|\psi\rangle$ describing the state of a finite number of qubits, there exists a LOCC (local operation and classical communication) measurement protocol that achieves the Cramér-Rao bound. However, in our current context, we are dealing with a wave packet that characterizes the state of a port. Therefore, the theorem cannot be applied directly. Here we introduce a modified version of the LOCC measurement protocol that can be applied to a multi-photon wave packet passing through a port. The central idea involves performing photon detection measurements repeatedly. Importantly, before each measurement, we pass the wave function through a beam splitter. The rotation parameters of this beam splitter, depend on the state $|\psi\rangle$, and the outcomes of previous measurements. Precisely, the corresponding POVM is:

$$\begin{aligned}\big\langle E_{t_1,t_2,\cdots,t_N}^{\sigma_1,\sigma_2,\cdots,\sigma_N}\big| &= \langle 0|\,\big(e_{t_1,t_2,\cdots,t_N}^{\sigma_1,\sigma_2,\cdots,\sigma_N}\big)\cdots\big(e_{t_1,t_2}^{\sigma_1,\sigma_2}\big)\big(e_{t_1}^{\sigma_1}\big),\\ &= \langle 0|\,\big(f_{t_1,t_2,\cdots,t_N}^{\sigma_1,\sigma_2,\cdots,\sigma_N}a_{t_N} + g_{t_1,t_2,\cdots,t_N}^{\sigma_1,\sigma_2,\cdots,\sigma_N}b_{t_N}\big)\cdots\big(f_{t_1,t_2}^{\sigma_1,\sigma_2}a_{t_2} + g_{t_1,t_2}^{\sigma_1,\sigma_2}b_{t_2}\big)\big(f_{t_1}^{\sigma_1}a_{t_1} + g_{t_1}^{\sigma_1}b_{t_1}\big).\end{aligned} \tag{F.2}$$

where $t_1,\cdots,t_N$ denote the times at which photon detections occur, $\sigma_i \in \{0,1\}$, and fs and gs are coefficients that we will specify later. Here, $e_{t_1,t_2,\cdots,t_i}^{\sigma_1,\sigma_2,\cdots,\sigma_i}$ represents the measurement operator for the beam splitter and photon detection, when measuring the i-th photon at time t_i. Note that $\sigma_1,\cdots,\sigma_{i-1}$ are fixed based on the results of the previous measurements, and σ_i can take on values of either 0 or 1 based on the measurement outcome. When we demand that these single-photon measurements be complete within the subspace of one excitation, we arrive at the following expression:

$$\Big|e_{t_1,t_2,\cdots,t_i}^{\sigma_1,\sigma_2,\cdots,\sigma_{i-1},0}\Big\rangle\Big\langle e_{t_1,t_2,\cdots,t_i}^{\sigma_1,\sigma_2,\cdots,\sigma_{i-1},0}\Big| + \Big|e_{t_1,t_2,\cdots,t_i}^{\sigma_1,\sigma_2,\cdots,\sigma_{i-1},1}\Big\rangle\Big\langle e_{t_1,t_2,\cdots,t_i}^{\sigma_1,\sigma_2,\cdots,\sigma_{i-1},1}\Big| = a_{t_i}^\dagger\,|0\rangle\langle 0|\,a_{t_i} + b_{t_i}^\dagger\,|0\rangle\langle 0|\,b_{t_i} = I_1,$$

where, $\langle e_{\mathbf{t}}^{\boldsymbol{\sigma}}| = \langle 0|\,e_{\mathbf{t}}^{\boldsymbol{\sigma}}$. This condition implies that the matrix $\begin{pmatrix} f_{t_1,t_2,\cdots,t_i}^{\sigma_1,\sigma_2,\cdots,\sigma_{i-1},0} & f_{t_1,t_2,\cdots,t_i}^{\sigma_1,\sigma_2,\cdots,\sigma_{i-1},1} \\ g_{t_1,t_2,\cdots,t_i}^{\sigma_1,\sigma_2,\cdots,\sigma_{i-1},0} & g_{t_1,t_2,\cdots,t_i}^{\sigma_1,\sigma_2,\cdots,\sigma_{i-1},1}\end{pmatrix}$ need to be unitary. Using this relation, we can show that the measurement operators defined in Eq. [F.2] are complete,

$$\sum_N\sum_{\vec{\boldsymbol{\sigma}}_N}\int\cdots\int\big|E_{t_1,t_2,\cdots,t_N}^{\sigma_1,\sigma_2,\cdots,\sigma_N}\big\rangle\,\big\langle E_{t_1,t_2,\cdots,t_N}^{\sigma_1,\sigma_2,\cdots,\sigma_N}\big|\;dt_1\ldots dt_N = I.$$

The next step is to show that under what conditions, the coefficients fs and gs are either 0 or 1 if we ask the measurements satisfy the expression in Eq. [F.1], and consequently, saturate the Cramer-Rao bound. We can find these values at the first step by the following procedure:

—Zeroth step: M should satisfy $\langle 0|\, M\, |0\rangle = 0$. By defining $h = \langle \psi|\, H\, |\psi\rangle$ and $|\phi\rangle = H\, |\psi\rangle$, this condition can be written as:

$$\begin{aligned} 2h|\langle 0|\, \psi\rangle|^2 - \langle 0|\, \psi\rangle \langle \phi|\, 0\rangle - \langle \psi|\, 0\rangle \langle 0|\, \phi\rangle = 0, \\ \rightarrow h|\langle 0|\, \psi\rangle|^2 = 0, \end{aligned} \tag{F.3}$$

where we used $H\, |0\rangle = 0$.

—First step: We begin by finding $|E_{t_1}\rangle$ such that $\langle E_{t_1}|\, M\, |E_{t1}\rangle = 0$. This requirement can be expressed as:

$$\langle E_{t_1}|\, \phi\rangle \langle \psi|\, E_{t_1}\rangle + \text{c.c.} - 2h \langle E_{t_1}|\, \psi\rangle \langle \psi|\, E_{t_1}\rangle = 0.$$

We can rewrite the above equation as:

$$\begin{pmatrix} f_{t_1} & g_{t_1} \end{pmatrix} \varLambda^{(1)} \begin{pmatrix} f^*_{t_1} \\ g^*_{t_1} \end{pmatrix} = 0, \tag{F.4}$$

where $\varLambda$ is a 2 by 2 hermitian matrix with diagonal elements given by:

$$\begin{aligned} \lambda^{(1)}_{00} &= \Big(\langle 0|\, a_{t_1}\, |\phi\rangle \langle \psi|\, a_{t_1}\, |0\rangle + \text{c.c.} \Big) - 2h \langle 0|\, a_{t_1}\, |\psi\rangle \langle \psi|\, a_{t_1}\, |0\rangle\,, \\ \lambda^{(1)}_{11} &= \Big(\langle 0|\, b_{t_1}\, |\phi\rangle \langle \psi|\, b_{t_1}\, |0\rangle + \text{c.c.} \Big) - 2h \langle 0|\, b_{t_1}\, |\psi\rangle \langle \psi|\, b_{t_1}\, |0\rangle\,. \end{aligned}$$

Moreover, we can show that:

$$\begin{aligned} \langle 0|\, a_{t_1}\, |\phi\rangle &= \langle 0|\, a_{t_1} H\, |\psi\rangle = i \langle 0|\, b_{t_1}\, |\psi\rangle\,, \\ \langle 0|\, b_{t_1}\, |\phi\rangle &= \langle 0|\, b_{t_1} H\, |\psi\rangle = -i \langle 0|\, a_{t_1}\, |\psi\rangle\,, \end{aligned}$$

To be able to find two sets of f and g such that they satisfy Eq.[F.4], the matrix $\varLambda$ needs to be traceless.

$$\begin{aligned} \lambda^{(1)}_{00} &= i\Big(\langle 0|\, a_{t_1}\, |\psi\rangle \langle \psi|\, b^\dagger_{t_1}\, |0\rangle - \langle 0|\, b_{t_1}\, |\psi\rangle \langle \psi|\, a^\dagger_{t_1}\, |0\rangle \Big) - 2h|\psi(t_1, \emptyset)|^2 = -2\,\text{Im}\,\big(\psi(t_1, \emptyset)\psi^*(\emptyset, t_1)\big) - 2h|\psi(t_1, \emptyset)|^2, \\ \lambda^{(1)}_{11} &= i\Big(- \langle 0|\, b_{t_1}\, |\psi\rangle \langle \psi|\, a^\dagger_{t_1}\, |0\rangle + \langle 0|\, a_{t_1}\, |\psi\rangle \langle \psi|\, b^\dagger_{t_1}\, |0\rangle \Big) - 2h|\psi(\emptyset, t_1)|^2 = -2\,\text{Im}\,\big(\psi(t_1, \emptyset)\psi^*(\emptyset, t_1)\big) - 2h|\psi(\emptyset, t_1)|^2, \\ \implies \lambda^{(1)}_{00} + \lambda^{(1)}_{11} &= -4\,\text{Im}\,\big(\psi(t_1, \emptyset)\psi^*(\emptyset, t_1)\big) - 2h\Big(|\psi(t_1, \emptyset)|^2 + |\psi(\emptyset, t_1)|^2 \Big), \end{aligned}$$

where we defined:

$$\psi(\tau_a, \tau_b) = \langle 0| \prod_{t \in \tau_a} a_t \prod_{t' \in \tau_b} b_{t'}\, |\psi\rangle\,,$$

for arbitrary sets of times τ_a, and τ_b. Therefore, the condition for the beam splitter and photodetection to be optimal is:

$$2\,\text{Im}\,\big(\psi(t_1, \emptyset)\psi^*(\emptyset, t_1)\big) + h\Big(|\psi(t_1, \emptyset)|^2 + |\psi(\emptyset, t_1)|^2 \Big) = 0. \tag{F.5}$$

If the above condition is true and if $|\psi(t_1, \emptyset)| = |\psi(\emptyset, t_1)|$, then $\lambda_{00}^{(1)}$ and $\lambda_{11}^{(1)}$ are both equal to zero. Therefore, the two sets of f and g can be chosen as:

$$\begin{pmatrix} f_{t_1} \\ g_{t_1} \end{pmatrix} = \begin{pmatrix} 1 \\ 0 \end{pmatrix} \text{ or } \begin{pmatrix} 0 \\ 1 \end{pmatrix}.$$

And therefore, photodetection can be optimal at the first step.

—Second step: The condition for the second measurement to be optimal is $\langle E_{t_1,t_2}| M |E_{t_1,t_2}\rangle = 0$. This can be written as:

$$\begin{pmatrix} f_{t_1,t_2} & g_{t_1,t_2} \end{pmatrix} \Lambda^{(2)} \begin{pmatrix} f^*_{t_1,t_2} \\ g^*_{t_1,t_2} \end{pmatrix} = 0.$$

The first measurement outcome could be either a_{t_1} or b_{t_1}. If the first photodetection outcome is a_{t_1}, the the diagonal terms of the matrix $\Lambda^{(2)}$ are:

$$\begin{aligned} \lambda_{00}^{(2)} &= -2\,\mathrm{Im}\left(\left[\psi(t_1, t_2) + \psi(t_2, t_1)\right]\psi^*(t_1 t_2, \emptyset)\right) - 2h|\psi(t_1 t_2, \emptyset)|^2, \\ \lambda_{11}^{(2)} &= -2\,\mathrm{Im}\left(\left[\psi(\emptyset, t_1 t_2) - \psi(t_1 t_2, \emptyset)\right]\psi^*(t_1, t_2)\right) - 2h|\psi(t_1, t_2)|^2, \end{aligned}$$

then the condition for $\Lambda^{(2)}$ to be traceless can be written using the above equations. We can also get another condition assuming the first measurement outcome to be b_{t_1}. Therefore, if we ask photodetection and beamsplitters to be optimal for the second measurement, the the two conditions are:

$$\mathrm{Im}\Big(\left[\psi(t_1, t_2) + \psi(t_2, t_1)\right]\psi^*(t_1 t_2, \emptyset) + \left[\psi(\emptyset, t_1 t_2) - \psi(t_1 t_2, \emptyset)\right]\psi^*(t_1, t_2)\Big) + h\Big(|\psi(t_1 t_2, \emptyset)|^2 + |\psi(t_1, t_2)|^2\Big) = 0, \tag{F.6}$$

$$\mathrm{Im}\Big(\left[\psi(\emptyset, t_1 t_2) - \psi(t_1 t_2, \emptyset)\right]\psi^*(t_2, t_1) - \left[\psi(t_1, t_2) + \psi(t_2, t_1)\right]\psi^*(\emptyset, t_1 t_2)\Big) + h\Big(|\psi(\emptyset, t_1 t_2)|^2 + |\psi(t_2, t_1)|^2\Big) = 0. \tag{F.7}$$

If these conditions result in $\lambda_{00}^{(2)}$ and $\lambda_{11}^{(2)}$ to be equal to zero individually, then we can choose the basis for f, and g such that photodetection is optimal and there is no need for the beamsplitters. But that is not generally the case. In the next subsection, we give an example in which photodetection and beamsplitters are optimal but photodetection alone is not at the second step.

—Nth step: If we assume photodetection to be optimal for the first $N-1$ steps, then the measurement outcome can be written as the following projection (the values for f and g are either 1 or 0):

$$\left\langle E_{t_1,t_2,\cdots,t_{N-1}}\right| = \langle 0| \prod_{t\in\tau_a} a_t \prod_{t'\in\tau_b} b_{t'},$$

for a pair of disjoint sets τ_a and τ_b such that:

$$\tau_a \cup \tau_b = \{t_1, t_2, \cdots, t_{N-1}\}.$$

Now we ask what are the conditions for beam splitter and photodetection to be optimal at the Nth step. The condition for that is $\langle E_{t_1,\cdots,t_N}| M |E_{t_1,\cdots,t_N}\rangle = 0$, which can be written as:

$$\begin{pmatrix} f_{t_1,\cdots,t_N} & g_{t_1,\cdots,t_N} \end{pmatrix} \Lambda^{(N)} \begin{pmatrix} f^*_{t_1,\cdots,t_N} \\ g^*_{t_1,\cdots,t_N} \end{pmatrix} = 0,$$

with the diagonal terms:

$$\lambda^{(N)}_{00} = -2\,\mathrm{Im}\left(\Big[\sum_{t\in\tau_a\cup t_N} \psi(\tau_a \cup t_N \setminus t, \tau_b \cup t) - \sum_{t\in\tau_b} \psi(\tau_a \cup t_N \cup t, \tau_b \setminus t) \Big] \psi^*(\tau_a \cup t_N, \tau_b) \right) - 2h|\psi(\tau_a \cup t_N, \tau_b)|^2, \tag{F.8}$$

$$\lambda^{(N)}_{11} = -2\,\mathrm{Im}\left(\Big[\sum_{t\in\tau_a} \psi(\tau_a \setminus t, \tau_b \cup t_N \cup t) - \sum_{t\in\tau_b\cup t_N} \psi(\tau_a \cup t, \tau_b \cup t_N \setminus t) \Big] \psi^*(\tau_a, \tau_b \cup t_N) \right) - 2h|\psi(\tau_a, \tau_b \cup t_N)|^2. \tag{F.9}$$

The optimality condition is the sum of $\lambda^{(N)}_{00}$ and $\lambda^{(N)}_{11}$ to be zero. There are a total of 2^{N-1} optimality conditions for all possible pairs of τ_a and τ_b.

F.1 non-Identical sources in a product state

If we assume the sources initially in a product state, then we can write:

$$\psi(\tau_a, \tau_b) = f(\tau_a) g(\tau_b).$$

where:

$$f(\tau_a) = \langle 0| \prod_{t\in\tau_a} a_t |\psi_a\rangle, \quad g(\tau_b) = \langle 0| \prod_{t\in\tau_b} b_t |\psi_b\rangle$$

We study the optimal measurement conditions for photodetection and beamsplitters in two cases where (I) h is zero and $f(\tau)$, $g(\tau)$ are non-zero for any set τ, and (II) h is non-zero.

(I) $h = 0$ and $f(\tau)$, $g(\tau)$ are non-zero:

Eq.[F.3] is satisfied since $h = 0$ by assumption. The condition for the first measurement in Eq.[F.5] is:

$$\mathrm{Im}\left(\psi(t_1, \emptyset)\psi^*(\emptyset, t_1)\right) = \mathrm{Im}\left(f(t_1) g^*(t_1)\right) = 0,$$

which gives the condition that:

$$\theta(t_1) = \eta(t_1),$$

where we defined:

$$\theta(\tau_a) = \mathrm{Arg}(f(\tau_a)), \quad \eta(\tau_b) = \mathrm{Arg}(g(\tau_a)).$$

As previously mentioned if this condition is satisfied, then photodetection is optimal at the first step. For the second step the conditions in Eq.[F.6, F.7] can be simplified to:

$$\mathrm{Im}\left[Z\begin{pmatrix} f^*(t_1t_2) \\ g^*(t_1t_2) \end{pmatrix} e^{i\left(\theta(t_1)+\theta(t_2)\right)}\right] = 0.$$

where:

$$Z = \begin{pmatrix} 2|f(t_1)g(t_2)| + |f(t_2)g(t_1)| & -|f(t_1)g(t_2)| \\ -|f(t_2)g(t_1)| & 2|f(t_2)g(t_1)| + |f(t_1)g(t_2)| \end{pmatrix}$$

If the matrix Z, is invertible, then we get:

$$\theta(t_1t_2) = \eta(t_1t_2) = \theta(t_1) + \theta(t_2).$$

If this condition is satisfied, it is straightforward to see that $\lambda_{00}^{(2)}$, and $\lambda_{11}^{(2)}$ are equal to zero individually and therefore, photodetection alone is optimal. Determinant of Z, being zero, gives that:

$$|f(t_1)g(t_2)| = -|f(t_2)g(t_1)|$$

Which results in either $f(t)$ or $g(t)$ being zero for some values of time, which is a contradict since we assume f, and g to be non zero. For $N = 3$, one of the optimality conditions is:

$$\mathrm{Im}\left(\left[|2f(t_1t_2)g(t_3)| + |f(t_1t_3)g(t_2)| + |f(t_2t_3)g(t_1)|\right] f(t_1t_2t_3)e^{i(\theta(t_1)+\theta(t_2)+\theta(t_3))}\right),$$

which gives the condition:

$$\theta(t_1t_2t_3) = \theta(t_1) + \theta(t_2) + \theta(t_3),$$

And similarly the same condition can be achieved for $\eta(t_1t_2t_3)$. Using this result, we can see that $\lambda_{00}^{(3)}$, $\lambda_{11}^{(3)}$ are zero individually in all cases at step three. Therefore, again photodetection is optimal at this step. This gives the idea that for the case of initial product states for the sources, photodetection can be optimal and there is no need for the adjustable beam splitters. We prove this statement using induction. We assume the induction statement as following: For any two pairs of disjoint sets $\{\tau_1, \tau_2\}$ and $\{\tau_1', \tau_2'\}$ such that $\tau_1 \cup \tau_2 = \tau_1' \cup \tau_2' = \tau_N$ and $\tau_N = \{t_1, \cdots, t_N\}$, we have:

$$\theta(\tau) = \eta(\tau), \quad \theta(\tau_1) + \theta(\tau_2) = \theta(\tau_1') + \theta(\tau_2'), \tag{F.10}$$

where $\theta(\tau)$ ($\eta(\tau)$) is the phase of the complex number $f(\tau)(g(\tau))$. First we show that this condition is equivalent to photodetection being optimal at step N. For this we need to show that Eq. [F.8, F.9] will be zero. Using Eq. [F.10], each term in the summations of $\lambda_{00}^{(N)}$, and $\lambda_{11}^{(N)}$ is equal to zero and therefore, the induction statement results in photodetection being optimal. As we have shown the statement being true for the base case of $N = 3$, we just need to prove the statement for $N = k$, assuming: (1) the induction statement (Eq.[F.10]) to be true for

$N < k$, and (2) photodetection and beam splitter being optimal for $N = k$ (i.e. $\lambda_{00}^{(k)} + \lambda_{11}^{(k)} = 0$ for all possible pairs of τ_a, and τ_b).

First by just using assumption (1), we show that if the set sizes $|\tau_1|, |\tau_2|, |\tau_1'|, |\tau_2'| < k$, then the induction statement for $N = k$ can be achieved. we can write:

$$\tau_1 \cup \tau_2 = \tau_1' \cup \tau_2' = \{t_1, \cdots, t_k\},$$

$$\begin{aligned}\rightarrow \theta(\tau_1) + \theta(\tau_2) &= \theta(\tau_1 \cap \tau_1') + \theta(\tau_1 \cap \tau_2') + \theta(\tau_2 \cap \tau_1') + \theta(\tau_2 \cap \tau_2') \\ &= \Big(\theta(\tau_1 \cap \tau_1') + \theta(\tau_2 \cap \tau_1')\Big) + \Big(\theta(\tau_1 \cap \tau_2') + \theta(\tau_2 \cap \tau_2')\Big) = \theta(\tau_1') + \theta(\tau_2'),\end{aligned}$$

where we used $\theta(\emptyset) = 0$, and assumption (1). Next step we use assumption (2) and show that the induction statement is true when $\tau_1 = \tau_k$, and $\tau_2 = \emptyset$. We start by choosing $\tau_a = \tau_{k-1} \setminus \{t_l\}$, $\tau_b = \{t_l\}$, where $\tau_{k-1} = \{t_1, \cdots, t_{k-1}\}$, and $0 < l < k$. Therefore, if $k > 3$, we can write:

$$\begin{aligned}\lambda_{00}^{(k)} &= 2\,\mathrm{Im}\Big(f(\tau_a \cup t_k \cup t_l) g(\emptyset) f^*(\tau_a \cup t_k) g^*(t_l)\Big), \\ \lambda_{11}^{(k)} &= 0,\end{aligned}$$

Therefore, we get the condition that:

$$\theta(\tau_k) = \theta(t_l) + \theta(\tau_k \setminus t_l) \quad 0 < l < k.$$

As a result we can conclude that the induction statement for $N = k$ is true and therefore, photodetection is optimal for identical sources with same initial states.

(II) $h \neq 0$ **:**

The optimality condition at the zeroth step gives that:

$$|f(\emptyset)g(\emptyset)| = 0,$$

Using this, the conditions at the first step can be written as:

$$|f(t_1)g(\emptyset)|^2 + |f(\emptyset)g(t_1)|^2 = 0 \rightarrow |f(t_1)g(\emptyset)| = 0 \text{ and } |f(\emptyset)g(t_1)| = 0.$$

Next, the condition at the second step becomes:

$$|f(t_1t_2)g(\emptyset)|^2 + |f(t_1)g(t_2)|^2 = 0 \quad \text{and} \quad |f(\emptyset)g(t_1t_2)|^2 + |f(t_2)g(t_1)|^2 = 0$$

$$\rightarrow |f(t_1t_2)g(\emptyset)| = 0,\ |f(t_1)g(t_2)| = 0, \text{ and } |f(\emptyset)g(t_1t_2)| = 0.$$

Similarly, the optimal conditions give that for any two set τ_a, and τ_b, we have:

$$|f(\tau_a)g(\tau_b)| = 0.$$

This implies that either $|\psi_a\rangle = 0$, or $|\psi_b\rangle = 0$ which is not physical. Therefore, optimality of photodetection and beam splitters, implies that h needs to be zero.

F.2 Counterexample: entangled state

Consider a two-photon wavepacket such that:

$$\psi(t_1t_2,\emptyset) = f(t_1,t_2), \quad \psi(t_1,t_2) = -f(t_1,t_2), \quad \psi(\emptyset,t_1t_2) = (1+i)f(t_1,t_2), \quad \psi(t_2,t_1) = (1+i)f(t_1,t_2),$$

where the function $f(t_1,t_2)$ should be chosen such that the wave function is normalized. First we note that for this specific example, h is equal to zero, and the conditions in Eq.[F.3] and Eq.[F.5] are satisfied since it's a two photon wavepacket. It's straight forward to check that the conditions in [F.6, F.7] are also satisfied and therefore, beamsplitter and photodetection is optimal. However, $\lambda_{00}^{(2)}$ and $\lambda_{11}^{(2)}$ are not zero for both cases of measurement outcomes in the first photodetection. Therefore, photodetection alone is not optimal and we need the linear optics to saturate the cramer-rao bound.